Ultrafast Joule heating method for synthesizing CoNi nanoalloy catalysts for electrocatalytic hydrogen evolution

Hanqing Yu, Jianyu Li, Ni Yang, Dan Zhao, Bo Yang, Yanqing Hou, Gang Xie

PII: S0925-8388(25)00659-0

DOI: https://doi.org/10.1016/j.jallcom.2025.179101

Reference: JALCOM179101

To appear in: *Journal of Alloys and Compounds*

Received date: 17 December 2024
Revised date: 2 February 2025
Accepted date: 8 February 2025

Please cite this article as: Hanqing Yu, Jianyu Li, Ni Yang, Dan Zhao, Bo Yang, Yanqing Hou and Gang Xie, Ultrafast Joule heating method for synthesizing CoNi nanoalloy catalysts for electrocatalytic hydrogen evolution, *Journal of Alloys and Compounds,* (2025) doi:https://doi.org/10.1016/j.jallcom.2025.179101

Ultrafast Joule heating method for synthesizing CoNi nanoalloy catalysts for electrocatalytic hydrogen evolution

AUTHOR NAMES：Hanqing Yu [1,†], Jianyu Li[2,†], Ni Yang [3,4†], Dan Zhao [2], Bo Yang[1,4*] ,Yanqing Hou [2,*] and Gang Xie [3,4*]

AUTHOR ADDRESS:

[1]Guizhou Key Laboratory of Advanced Computing, Guizhou Normal University, Guiyang 550014, China

[2]Faculty of Metallurgy and Energy Engineering, Kunming University of Science and Technology, Kunming 650093, China

[3]Kunming Metallurgical Research Institute, Kunming 650093, China

[4]State Key Laboratory of Advanced Metallurgy for Non-ferrous Metals，Kunming 650093, China

***** Correspondence: gznuyangbo@163.com (B.Y.); hhouyanqing@163.com (Y.H.); gangxie@sina.com (G.X.)

† These authors contributed equally to this work.

Abstract

The hydrogen evolution reaction (HER) is a critical electrochemical reaction in water splitting. However, existing noble metal catalysts tend to aggregate and dissolve under acidic conditions, resulting in low preparation efficiency, poor catalytic activity,

and stability. To address this issue, this study employed an ultrafast Joule heating (UJH) technique to rapidly synthesize a cobalt-nickel nanoalloy heterostructure supported on carbon cloth (Co-Ni@CC) and tested its performance in electrocatalytic HER under acidic conditions. The study demonstrated that the metallic heterostructure of Co and Ni nanocrystals on a conductive carbon cloth substrate exhibited excellent dispersion, significantly increasing the contact area of active sites and delivering superior electrocatalytic performance (η 10 = 231 mV, 111.7mV dec^{-1}). With its high catalytic activity, low cost, good electrical conductivity, and chemical stability, Co-Ni@ CC represents an ideal alternative to noble metal catalysts. Furthermore, this study demonstrates the potential of the UJH technique for rapidly constructing high-performance metal heterostructures, offering a new approach for developing electrocatalysts for overall water splitting.

Keywords: Ultrafast Joule heating , Electrocatalytic hydrogen evolution , Cobalt-nickel nanoalloys , Carbon cloth

Introduction

As a clean and sustainable energy carrier, hydrogen has emerged as a critical solution to the increasingly serious energy crisis and environmental pollution. Electrochemical water splitting offers an efficient, clean, and carbon-free method for hydrogen production, in which the hydrogen evolution reaction (HER) serves as the pivotal step[1]. However, the sluggish reaction kinetics of HER often result in considerable energy losses, significantly limiting the practical application of water electrolysis for hydrogen generation. Consequently, developing efficient and cost-effective HER electrocatalysts has become an urgent research priority[2]. An ideal HER electrocatalyst should demonstrate not only a low overpotential but also low cost, ease of fabrication, and excellent long-term stability[3]. Therefore, developing catalysts and preparation methods that effectively enhance the efficiency of HER is crucial for achieving high-performance electrolyzer operation and practical applications.

Although platinum and other noble metals exhibit the highest HER performance and the lowest overpotential, their exorbitant cost restricts their practical applications[4][5]. In recent years, intensive studies have focused on efficient non-noble-metal-based materials as HER electrocatalysts, among which transition-metal-based materials have garnered considerable attention[6][7][8]. Among all transition metals, cobalt and nickel have been widely investigated owing to their low cost and high catalytic activity toward the hydrogen evolution reaction[9][10][11]. However, Co- and Ni-based catalysts often suffer from limited activity and stability due to low electrical conductivity and suboptimal binding energies of hydrogen intermediates, preventing

them from achieving ideal performance. Therefore, combining cobalt and nickel via alloy formation can effectively tune their d-band center, facilitating faster electron transfer and thus promoting the HER[12]. In addition, alloying not only aids in enhancing the chemical stability of both metals in acidic or alkaline electrolytes but also reduces reaction resistance, thereby improving overall catalytic efficiency.

However, the high-temperature annealing process commonly used to fabricate traditional alloys can alter catalyst morphology, lead to catalyst agglomeration, reduce the exposure of active sites, and ultimately diminish stability during reactions. Joule heating technology is an emerging material processing technique[13]. During the alloying process, an instantaneous high current is applied to generate extremely high temperatures, enabling rapid melting, diffusion, and reduction of metallic precursors within milliseconds. This is followed by an extremely fast quenching and annealing process. Under these conditions, the swift mixing of the molten metal and efficient quenching form alloy nanoparticles with nanoscale dispersion[14]. For example, Qiu et al.[15] synthesized an Ag/Co/C composite electrocatalyst for the oxygen reduction reaction (ORR) via flash Joule heating of Ag and Co. Under flash evaporation Joule heating and quenching, the large immiscible gap in the liquid Ag-Co alloy prevented the formation of a solid solution. In alkaline media at 0.8 V vs. RHE, the composite catalyst exhibited a specific activity 40 times higher than that of the original Ag/C and a mass activity 52 times greater. Li et al.[16] employed flash Joule heating to prepare a bifunctional Ru-Cu@CM/CC electrocatalyst for both HER and OER, featuring ultrafine Cu and Ru alloy heterostructures confined within a carbon matrix. This

catalyst exhibited outstanding performance in both alkaline and acidic media, surpassing Pt/C and RuO_2. Moreover, Li et al.[17] fabricated NiRu alloy nanoparticles with strong metal-support interactions via flash Joule heating, demonstrating remarkable HER activity in alkaline solution, with an overpotential of only 5.1 mV at 10 mA cm^{-2} and excellent stability over 10 hours. Evidently, constructing alloy heterostructures can optimize the adsorption and desorption processes of intermediates and modulate the binding energies, thereby enhancing electrocatalytic activity[18][19][20]. Despite the promising electrocatalytic performance of these materials, they all rely on noble metals as the primary substrate and still face obstacles that must be overcome. For instance, under prolonged cycling tests, these nanoparticles can readily aggregate into larger clusters, and some nanoparticles are susceptible to corrosion and dissolution in acidic media. Consequently, finding a stable support to prevent nanoparticle aggregation and dissolution while increasing the surface area is imperative. Owing to its high conductivity, large specific surface area, and exceptional chemical stability, carbon cloth provides significant advantages in improving charge-transfer efficiency, exposing catalytic active sites, and maintaining long-term stability[21][22]. Hence, selecting an appropriate strategy to fabricate low-cost, easily produced, and long-term stable HER electrocatalysts is particularly crucial.

This study presents an innovative UJH strategy for preparing cobalt–nickel (Co–Ni) nanoalloy catalysts supported on carbon cloth (Co–Ni@CC) within just a few milliseconds. During this process, a carbothermal reduction reaction converts Co and Ni compounds on the carbon substrate into metallic cobalt and nickel, while a transient

high temperature of 2000 K enables rapid alloying and formation of heterostructures. The Co–Ni alloy heterostructures fabricated via the UJH method exhibit excellent dispersion and stability on the carbon cloth substrate, significantly increasing the accessible area of active sites and optimizing the adsorption and desorption behaviors of intermediates. This study not only demonstrates the potential of the UJH method for fabricating highly efficient electrocatalysts but also shows that the resulting Co–Ni@CC catalyst achieves remarkable catalytic performance in acidic conditions, including lower overpotential, excellent charge-transfer resistance, and high stability over extended cycling. This innovative fabrication strategy offers new insights for designing efficient, stable, and cost-effective HER electrocatalysts, thereby advancing the practical industrial applications of non-precious metal electrocatalysts.

2. Experimental

2.1. Materials

Cobalt(II) chloride hexahydrate ($CoCl_2 \cdot 6H_2O$, analytical reagent (AR)), nickel(II) chloride hexahydrate ($NiCl_2 \cdot 6H_2O$, 99%), sulfuric acid (H_2SO_4, 99%), and ethanol (C_2H_5OH) were all purchased from Shanghai Aladdin Biochemical Technology Co., Ltd. All the aforementioned chemicals were used directly without further purification. CC was purchased from FuelCellStore and was washed in 0.1 mol • L H_2SO_4 under ultrasonic conditions, followed by multiple rinses with deionized water and subsequent vacuum drying before use.

2.2 Synthesis of Co_x-Ni_y@ CC Electrocatalyst

A 1.5 cm × 1.0 cm piece of carbon cloth was immersed in a series of ethanol solutions of metal precursors with a total concentration of 0.1 M. These precursor solutions contained different concentrations of $CoCl_2$ and $NiCl_2$ and were named Co_x-Ni_y (where x and y represent the Co-to-Ni ratio of 1:0, 1:1, and 0:1). After soaking for 1 hour, the carbon cloth was dried in a vacuum drying oven at 150°C for 12 hours. The resulting product was then placed in an UJH apparatus under argon protection for instantaneous discharge. The discharge process involved a 30V, 0.5-second pretreatment to remove oxygen from the carbon cloth surface and enhance its conductivity, followed by a 120V, 1-second instantaneous discharge to obtain the Co_x-Ni_y@CC electrocatalyst samples.

2.3 Material Characterization

The morphology of Co_x-Ni_y@CC was characterized using TEM (Tecnai G2 F20,

FEI) and SEM (SU-8600, Hitachi) at different accelerating voltages. Co_x-Ni_y@CC was characterized using a confocal Raman spectrometer (WITec GmbH, Alpha 300R), an X-ray photoelectron spectrometer (Scientific K-Alpha, Thermo), and an X-ray diffractometer (Ultima IV, Rigaku). The X-ray photoelectron spectrometer (Scientific K-Alpha, Thermo) was used for additional characterization. Electrochemical performance tests were conducted using a DH7001D electrochemical workstation. The X-ray diffraction patterns were obtained within a 2θ range of 5–90° using Cu Kα radiation (λ = 1.54056 Å). The confocal Raman spectrometer was equipped with a TEM single-frequency laser (λ = 532 nm, laser power = 40 mW, WITec GmbH, Germany).

2.4 Electrochemical Performance Characterization

The HER was conducted at room temperature in a three-electrode electrochemical cell. The prepared 1 cm^2 carbon cloth sample was used as the working electrode. A 0.5 M H_2SO_4 solution was used as the electrolyte to evaluate HER activity, with an Ag/AgCl reference electrode and a platinum counter electrode serving as the reference and counter electrodes, respectively. Cyclic voltammetry (CV) was performed in Ar-saturated 0.5 M H_2SO_4 at a scan rate of 200 mV/s from 0.1 to 0.9 V vs. RHE to clean and activate the electrodes. The oxidation/reduction potential of the material was determined by cycling three times from 0 to 1.4 V vs. RHE at a scan rate of 20 mV/s. All obtained electrode potentials were referenced to the reversible hydrogen electrode (RHE), with an addition of (0.059 × pH + 0.098) V. Long-term stability was tested by cycling 1000 times in 0.5 M H_2SO_4 at a scan rate of 50 mV/s from 0.1 to 0.9 V vs. RHE, and the results were compared with the initial curve.

3. Results and Discussion

3.1 Microstructure and Phase Composition of the Catalyst

The size and composition of bimetallic nanoparticles significantly affect their electronic structure, which directly determines their electrocatalytic performance in HER [23][24]. As shown in Figure 1, a unique heterostructure of metallic Co and Ni (Co-Ni@ CC) can be prepared on CC through a straightforward experimental procedure. First, CC was immersed in ethanol solutions of metal precursors $CoCl_2$ and $NiCl_2$, followed by vacuum drying at 150°C to form $CoCl_2$ and $NiCl_2$ clusters on its surface. Finally, the CC loaded with Co and Ni metal particles was placed in an UJH apparatus under argon protection for millisecond-level UJH to achieve thermal reduction. The instantaneous high temperature above 2000 K caused the Co and Ni metal particles on the CC surface to undergo "fission" and "fusion," forming a uniform mixture of the two elements on the CC surface. During this process, CC was graphitized by the high temperature, increasing its conductivity. Finally, a phase-separated Co-Ni alloy heterostructure (Co-Ni@CC) was formed on the CC surface during the transient cooling process of 1 ms.

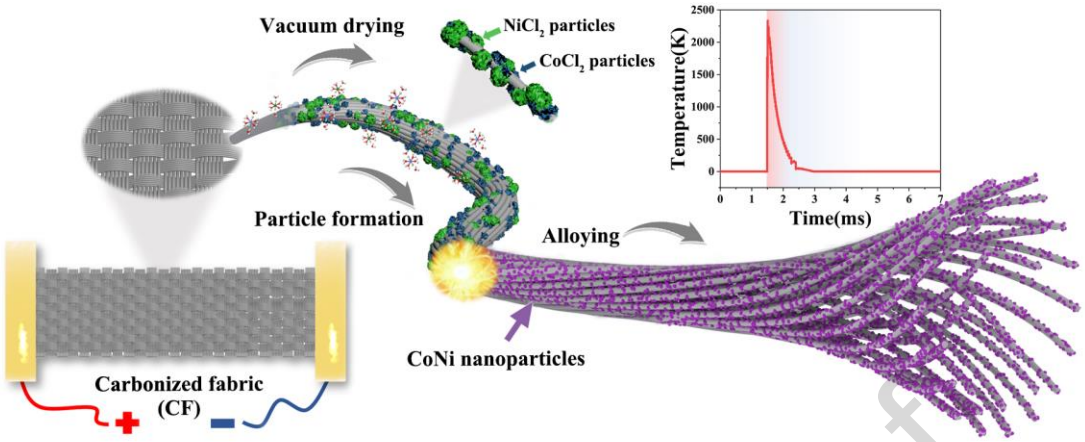

Figure 1. Schematic of UJH synthesis of Co-Ni@CC, with an inset showing the temperature variation during discharge.

The structure of Co-Ni@CC was characterized using scanning electron microscopy (SEM) and transmission electron microscopy (TEM). As shown in Figure 2, the SEM images reveal that CC without metal loading exhibits a relatively smooth surface (Figure 2a). After cleaning with 0.1mol•L H_2SO_4, microscopic etching forms on the CC surface (Figure 2b), thereby increasing the surface roughness. This roughening increases the specific surface area, providing more active sites, which is beneficial for the subsequent loading of $CoCl_2$ and $NiCl_2$ metal particles [25]. After UJH of CC soaked with different metal particles, the SEM images of Co_1-Ni_0@CC and Co_0-Ni_1@CC (Figure 2c and 2d) show well-defined nanoparticles. Although inconsistencies in the sizes of the nanoparticles were observed, they were uniformly coated on the CF, with no significant agglomeration or unloaded areas. Notably, Co-Ni@CC exhibits a morphology similar to that of Co_1-Ni_0@CC and Co_0-Ni_1@CC, indicating that the simultaneous introduction of both elements does not affect the formation of Co-Ni on the CC surface (Figure 2e). Moreover, with the introduction of the second element, the sizes of the heterostructured nanoparticles become more consistent and evenly

distributed on the CC surface, with no apparent phase separation (Figure S1). TEM was used to investigate the microscopic morphological changes during the UJH process. As shown in Figures 3a and 3b, the CoNi nanocrystals on the CC are larger than the original Co and Ni crystals, with particles averaging 20 ± 15 nm uniformly dispersed on the CC surface, exhibiting good crystallinity. The HR-TEM image in Figure 3c shows a tightly integrated interface. The ultrafine CoNi nanocrystals dispersed on the CC exhibit high crystallinity and clear lattice fringes. The lattice spacing of 2.04 Å corresponds to the (111) plane of the CoNi alloy, indicating the presence of a cobalt-nickel alloy in the particles. The X-ray energy dispersive spectroscopy (EDS) mapping (Figure 3d) reveals the presence of Co and Ni elements, confirming the retention of Co and Ni nanocrystals through UJH. Co and Ni elements are distributed at the same locations without isolated cobalt or nickel regions, indicating that Co and Ni jointly form an alloy (Figure 3e and 3f). These results indicate that the close interaction between the loaded nanoparticles and the CC enables rapid electron transfer between the reactants and the conductive substrate, thereby promoting electrocatalytic reactions. Notably, the heterostructures formed during the UJH process exhibit good dispersion, which is expected to increase the exposure of HER-active species.

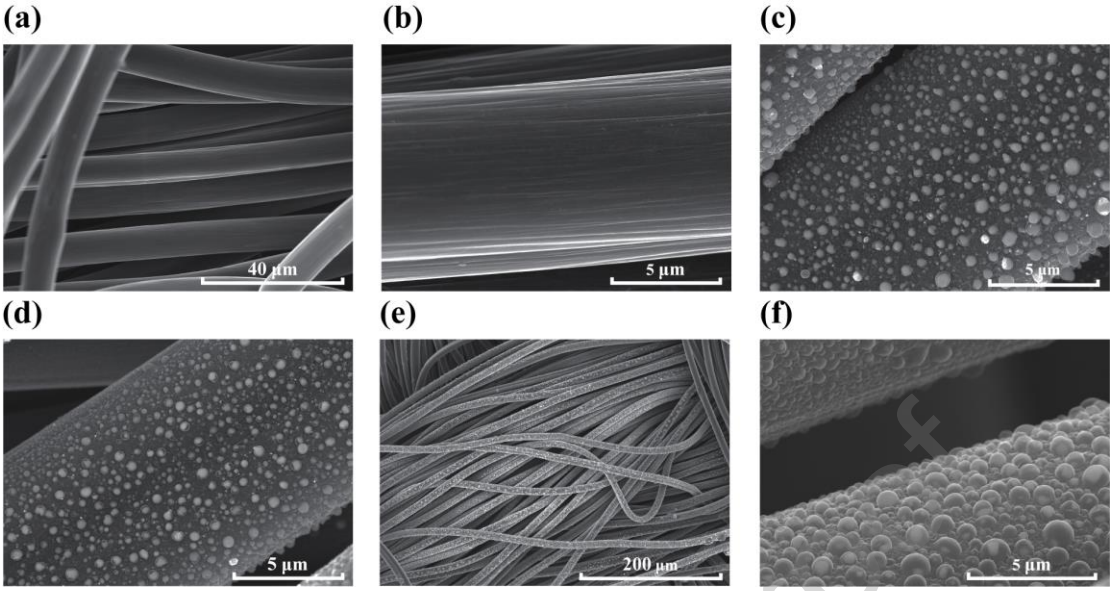

Figure 2. Morphology characterization. (a, b) CC cleaned with 0.1mol•L H_2SO_4. (c) SEM image of Co_1-Ni_0@CC. (d) SEM image of Co_0-Ni_1@CC. (e, f) SEM images of Co-Ni@CC.

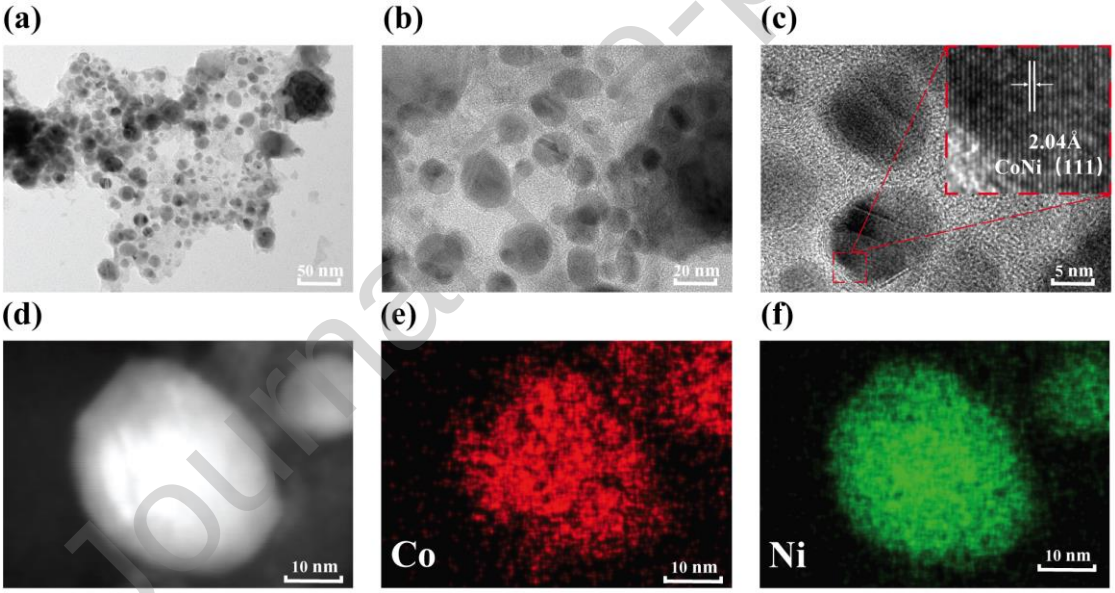

Figure 3. Microstructure characterization. (a, b) TEM images of Co-Ni@CC. (c) HR-TEM image of Co-Ni@CC. (d, e, f) HAADF-STAM images and corresponding EDS mappings of Co-Ni@CC.

The crystal phase of nanoparticles on CC was analyzed using X-ray diffraction (XRD). In the XRD spectrum of Figure 4a, for Co_x-Ni_y@CC, two prominent peaks appear at 26.4° and 54.5°, corresponding to the (002) and (004) planes of graphitized carbon (JCPDS No. 41-1487). For Co_1-Ni_0@CC, two low-intensity peaks are observed at 44.2° and 51.5°, corresponding to the (111) and (200) planes of Co (JCPDS card No.

97-004-4989). For Co_0-Ni_1@CC, two peaks can be detected at 45.5° and 53°, corresponding to the (111) and (200) planes of Ni (JCPDS card No. 97-004-1508). With the simultaneous addition of Co and Ni, the two characteristic peaks of Co and Ni shift to the left and right, indicating a decrease in the lattice spacing of the individual metals. Therefore, no Co- or Ni-based crystal peaks are detectable in the spectrum of Co-Ni@CC. Two new peaks appear at 44.3° and 51.7° between Co and Ni, which can be attributed to the (111) and (200) planes of the CoNi alloy. The XRD results indicate that the CoNi nanoparticles in Co-Ni@CC exhibit a single-phase alloy structure, and the shift in the XRD peak position aligns with the HRTEM lattice spacing analysis shown in Figure 3(c). Furthermore, Raman spectroscopy (Figure 4b) confirms that all Co_x-Ni_y@CC samples are free of metal oxide phases, which is consistent with the XRD results. Compared with the pristine carbon cloth before the reaction, distinct D and G bands are observed, and after the UJH process, a new 2D band appears at approximately 2,700 cm^{-1}. The Raman peak at 1,350 cm^{-1} indicates the presence of a disordered (D) band, while the graphite (G) band at 1,580 cm^{-1} represents the first-order scattering of the E_{2g} mode in sp^2 carbon domains. In addition, the appearance of the 2D band at 2,700 cm^{-1} suggests an enhanced degree of graphitization in the catalyst.

The X-ray photoelectron spectroscopy (XPS) test was used to characterize the chemical valence state of the elements on the surface of the material. All the XPS data were corrected with the C 1s (284.8 eV) standard peak. Figure 4c is the overall spectrum. The XPS measurement spectrum confirms the presence of C, O, Co and Ni elements on the surface of Co-Ni@CF. For the Co element in Co-Ni@CC, a characteristic peak

appears at 778.9 eV, corresponding to the Co 2p3/2 orbital (Figure 4d), which is associated with the valence state of Co in the CoNi alloy. Peaks at 781.4 eV, 794.3 eV, and 796.5 eV correspond to oxidized Co states, attributed to surface oxidation caused by exposure to the ambient atmosphere. Additional satellite peaks of Co 2p3/2 and 2p1/2 appear at 778.9 eV and 803 eV, respectively. Compared to the two characteristic peaks of Co 2p3/2 in Co_1-Ni_0@CC, the two peaks in Co-Ni@CC shift to the right by 0.6 eV, which is due to the change in Co binding energy caused by the formation of the CoNi alloy. This also demonstrates the strong electronic interaction between Co and Ni in the CoNi alloy. Similarly, in the XPS spectrum of Ni 2p shown in Figure 4e, the Ni 2p3/2 peak at 835.1 eV corresponds to the alloyed state of Ni in Co-Ni@CC, while other Ni 2p3/2 and Ni 2p1/2 peaks correspond to oxidized Ni states. The above results indicate the presence of an effective electronic coupling effect between Co and Ni. The electronic coupling effects between Co and Ni significantly influence the adsorption free energies of key reaction intermediates in the catalytic process by adjusting the d-band center positions of the metal alloy. For instance, the heterostructure of Co and Ni modulates the adsorption energy of H_{ads}, bringing it closer to zero and thereby reducing the overpotential required for the HER process. Furthermore, XPS analysis reveals noticeable shifts in the binding energies of Co and Ni, indicating strong electronic interactions within the heterostructure. This interaction optimizes the distribution of electrons and reaction pathways, thereby enhancing the kinetic efficiency of the HER[26][27]. The C 1s spectrum shown in Figure 4f features a peak at 284.88 eV corresponding to C=C double bonds or C-C single bonds and a peak at 283.88 eV

corresponding to sp2-hybridized carbon.

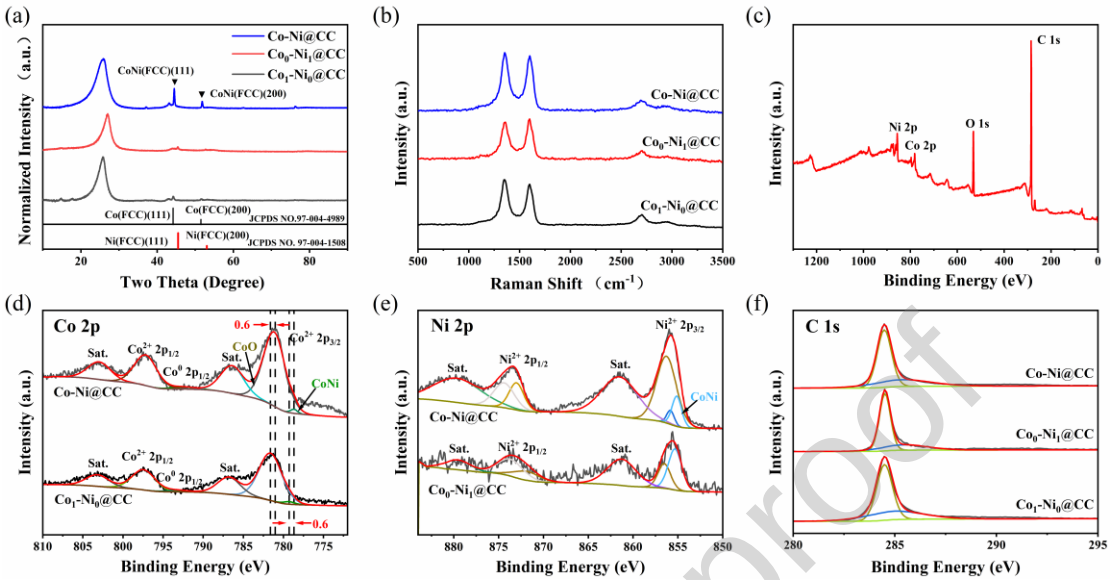

Figure 4. (a) XRD and (b) Raman spectra of Cox-Niy@CC. (c) XPS survey spectrum of Co-Ni@CC. (d) Peak fitting of Co 2p. (e) Peak fitting of Ni 2p. (f) Peak fitting of C 1s.

3.2 Electrochemical Performance of the Catalyst

Cobalt exhibits high stability and excellent hydrogen adsorption-desorption performance under acidic conditions, primarily due to its moderate hydrogen adsorption free energy (ΔG_H), which balances the adsorption and desorption of hydrogen on the electrode surface, effectively promoting the HER[28][29]. Nickel, as another important transition metal, exhibits exceptional catalytic activity in HER, particularly in the initial steps of water splitting, where it significantly accelerates electron transfer, reduces the reaction activation energy, and enhances the kinetic efficiency of the hydrogen evolution reaction [30].

The superior performance of cobalt-nickel composite materials arises from the synergistic effect between the two metals. Through alloying, cobalt-nickel composite materials are optimized in terms of structure, electronic properties, and surface adsorption energy. For example, alloying can tune the d-band center position, improve

the Fermi-level distribution, and provide the material with both cobalt's hydrogen adsorption-desorption capability and nickel's high electron transfer efficiency [31][32]. Furthermore, the heterogeneous interface plays a critical role in the HER process by modulating the adsorption energies of reaction intermediates H_{ads} and OH_{ads}, significantly reducing the activation energy barrier for HER. Characterization using XRD and HRTEM reveals that the Co-Ni alloy heterogeneous interface provides additional active sites with varying crystal orientations and electronic structures, thereby enhancing the adsorption and desorption behavior of intermediates. Additionally, the heterogeneous interface may introduce localized electric fields during the reaction, further accelerating the electron transfer rate[33].

Under acidic conditions, the synergistic interaction between Co and Ni significantly enhances the catalyst's corrosion resistance and long-term stability. The chemical stability of Co protects the metal matrix in strong acids, while the antioxidative properties of Ni effectively prevent the formation of surface oxide layers. The carbon cloth substrates produced via the UJH method further improve the electrode's durability and conductivity. Additionally, the lattice distortions and interfacial defects in the composite material further optimize the surface electron density distribution, enhancing the long-term stability and lifespan of the catalyst [34].

To demonstrate the advantages of the CC substrate-supported heterostructure obtained using the Joule heating strategy, the catalytic activity of Co-Ni@CC was evaluated. Electrochemical evaluation of the HER performance of Co_x-Ni_y@CC was conducted in 0.5M H_2SO_4 using a three-electrode configuration.

The linear sweep voltammetry (LSV) of Co_x-Ni_y@CC was tested in the voltage range of 0-0.5 V (HER) with a scan rate of 5 $mV \cdot s^{-1}$ and with iR correction applied. Based on the Tafel equation (Equation 3.1), the LSV data were processed to obtain the corresponding Tafel slope b [35]:

$$\eta = a + b \cdot log\ j \qquad (3.1)$$

In the equation, η is the overpotential, b is the Tafel slope, and j is the current density.

The LSV polarization curves of Co_x-Ni_y@CC are shown in Figure 5a, with Co_1-Ni_0@CC,Co_0-Ni_1@CC, and Co-Ni@CC used as reference samples. Compared to Co_x-Ni_y@CC samples, Co-Ni@CC exhibits a smaller overpotential in the potential range of 0-0.2 V. The overpotential at current densities of 10 mA cm^{-2} and 100 mA cm^{-2} is a critical indicator for HER electrocatalysts. As shown in Figure 5b, Co_1-Ni_0@CC and Co_0-Ni_1@CC exhibit poor HER activity, with large overpotentials of 370 mV and 416 mV at 10 mA cm^{-2}, respectively, and Co_0-Ni_1@CC showing an overpotential as high as 849 mV at 100 mA cm^{-2}. Notably, the overpotentials required for Co-Ni@CC to reach current densities of 10 mA cm^{-2} and 100 mA cm^{-2} are only 231 mV and 297 mV, respectively. This performance enhancement is primarily attributed to the electronic coupling effects and heterogeneous interfaces formed during the alloying process. These factors not only optimize the adsorption energies of reaction intermediates but also improve the overall charge transfer rate. In contrast, single-metal catalysts exhibit higher reaction impedance due to the lack of such synergistic effects. The reaction kinetics were evaluated by analyzing the rate-limiting step indicator, the Tafel slope. As shown in the Tafel plots in Figure 5c, the Tafel slopes of Co_1-Ni_0@CC, Co_0-Ni_1@CC,

and Co-Ni@CC are 216.9 mV dec^{-1}, 254.3 mV dec^{-1}, and 111.7 mV dec^{-1}, respectively. Compared to Co-Ni@CC, the HER activity of Co_1-Ni_0@CC and Co_0-Ni_1@CC is negligible. The electrochemically active surface area (ECSA) is one of the key indicators for evaluating HER catalytic performance. In this study, the double-layer capacitance (Cdl) method was employed to indirectly assess the ECSA. Figure S2 shows the cyclic voltammetry (CV) curves of Co_1-Ni_0@CC, Co_0-Ni_1@CC, and Co-Ni@CC at different scan rates within a potential window from 0.303 V (vs. RHE) to 1.101 V (vs. RHE). Based on the CV data, the slope of the linear fit between the current density (Δj) and the scan rate (ν) was used to determine Cdl, which was then used to calculate the ECSA according to ECSA = Cdl / $C_{dl,ideal}$. Here, $C_{dl,ideal}$ = 40 μF/cm^2 is a commonly referenced value of double-layer capacitance per unit area from the literature[36][37]. As shown in Figure 5d, the Cdl value of Co-Ni@CC is 11.38 mF·cm^{-2}, higher than that of Co_1-Ni_0@CC (10.45 mF·cm^{-2}) and Co_0-Ni_1@C C (8.34 mF·cm^{-2}). Correspondingly, the ECSA of Co-Ni@CC is calculated to be 284.5 cm^2, exceeding that of Co_1-Ni_0@CC (261.25 cm^2) and Co_0-Ni_1@CC (208.5 cm^2). The highest ECSA of Co-Ni@CC indicates the presence of more exposed active sites, which may be attributed to its small-sized metal heterostructure and structural optimization introduced by alloying. This finding further confirms the advantages of Co-Ni@CC in HER catalytic performance.

Co-Ni@CC exhibits excellent catalytic performance during the hydrogen evolution reaction (HER) in acidic media. Under acidic conditions, the hydrogen evolution reaction (HER) primarily consists of the following two steps:

(1) Volmer step (discharge step): In this step, water molecules dissociate on the electrode surface, forming adsorbed hydrogen (H_{ads}) and hydroxide ions [38]:

$$H_3O^+ + e^- \rightarrow H_{ads} + H_2O$$

In acidic media, the heterostructure of cobalt and nickel can effectively promote water dissociation, forming active hydrogen on the electrode surface.

(2) Heyrovsky or Tafel step: The generated adsorbed hydrogen further reacts to form hydrogen gas (H_2) [39]:

Heyrovsky step (electrochemical desorption):

$$H_{ads} + H_3O^+ + e^- \rightarrow H_2 + H_2O$$

Tafel step (chemical desorption):

$$H_{ads} + H_{ads} \rightarrow H_2$$

The heterostructure of cobalt and nickel provides optimized hydrogen adsorption energy in acidic solutions, facilitating the adsorption and desorption of hydrogen on the electrode surface[40]. Furthermore, this heterostructure exhibits strong corrosion resistance, maintaining high stability under acidic conditions, thereby enhancing catalytic activity and durability. This structure significantly accelerates the HER reaction rate, improving the overall electrocatalytic efficiency.

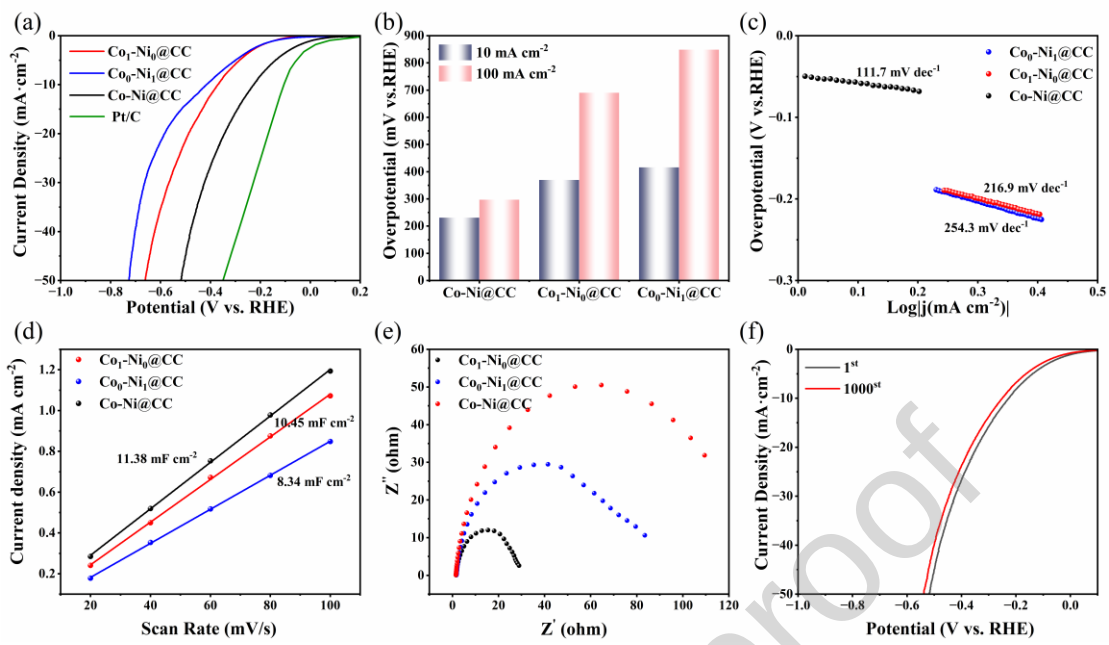

Figure 5. Electrocatalytic HER performance in 0.5M H_2SO_4. (a) HER LSV curves of Co_1-Ni_0@CC,Co_0-Ni_1@CC and Co-Ni@CC. (b) Comparison of overpotentials at 10 mA cm^{-2} and 100 mA cm^{-2} for Co_1-Ni_0@CC,Co_0-Ni_1@CC and Co-Ni@CC. (c) Corresponding Tafel plots of Co_1-Ni_0@CC,Co_0-Ni_1@CC and Co-Ni@CC. (d) Double-layer capacitance (Cdl) fitting curves of Co_1-Ni_0@CC,Co_0-Ni_1@CC and Co-Ni@CC. (e) Nyquist plots of Co_1-Ni_0@CC,Co_0-Ni_1@CC and Co-Ni@CC. (f) Polarization curves of Co-Ni@CC recorded before and after 1000 CV cycles.

Additionally, electrochemical impedance spectroscopy (EIS) was used to further investigate the charge transfer rate for electrochemical hydrogen production (Figure 5e). The charge transfer resistance (Rct) of Co-Ni@CC was 28.19 Ω, significantly lower than that of Co_1-Ni_0@CC (41.4 Ω) and Co_0-Ni_1@CC (64.6 Ω). The EIS results confirm that Co-Ni@CC possesses the fastest charge transfer capability at the electrode/electrolyte interface. This is attributed to the higher degree of graphitization and the heterostructure of the alloy in Co-Ni@CC, consistent with the results of the previous Raman and XRD tests. Therefore, the metallic heterostructure of Co and Ni nanocrystals can promote the adsorption and desorption of OH_{ads} and H_{ads} during the HER process, significantly optimizing the synergy between hydrogen adsorption and accelerating water dissociation, and contributing notably to the enhancement of

electrocatalytic performance[41]. Furthermore, the electrodes directly prepared on the conductive carbon cloth substrate facilitate efficient electron transfer during the catalytic reaction, promote electrolyte penetration, and expose active sites. Stability is another important indicator of catalytic performance. To determine the stability of the developed Co-Ni@CC, the hydrogen evolution polarization curves before and after 1000 CV cycles were compared, as shown in Figure 5f. The measured LSV curves show almost no change before and after CV cycles, indicating that Co-Ni@CC exhibits excellent stability. The samples after long-term HER testing were characterized by SEM. As shown in Figure S3, maintaining the favorable metal composition and morphological structure demonstrates the excellent stability of the prepared electrocatalyst.[42][43]. Another stability test was measured to observe the changes of the working curve of the material under constant voltage（Figure S4）. By using Co-Ni@CC as a working electrode to work at a constant voltage of 231 mVfor at least 30 h, as the reaction time increases, the current density was very stable and the loss was little, which also confirmed that Co-Ni@CC had great stability[44][45]. This remarkable long-term stability can be attributed to the tight adhesion of Co–Ni nanoalloys to the conductive substrate, with almost no detachment observed.

The above results demonstrate that Co-Ni@CC exhibits excellent electrocatalytic activity and highlight the effectiveness and rapidity of UJH in synthesizing electrocatalysts. For HER, heterostructures can modulate the adsorption and desorption of intermediates, while ultrafine nanoparticles provide a large number of exposed active sites, thereby facilitating accelerated reaction kinetics and enhancing electrocatalytic

performance. Furthermore, the carbon substrate can mitigate the agglomeration of these nanoparticles and metal heterostructures, contributing to robust electrocatalysts with outstanding stability.

4. Conclusion

Using the UJH method, we successfully and efficiently prepared a metal heterostructure in which Co and Ni nanocrystals are uniformly confined within the carbon cloth substrate. The developed Co-Ni@CC not only features ultrafine Co and Ni metal heterostructure active sites but also minimizes oxide formation during the alloying process on the carbon cloth, resulting in a superior alloy catalyst. This catalyst exhibits excellent electrocatalytic performance under acidic conditions ($\eta 10$=231mV, 111.7mV dec^{-1}). Benefiting from the UJH method, the Co-Ni alloy nanoparticles are uniformly embedded in the carbon cloth, which prevents them from detaching during the hydrogen evolution process, thereby maintaining excellent catalytic activity and stability. This work not only demonstrates the superior electrocatalytic performance of Co-Ni@CC but also provides a feasible approach for designing alloy catalysts using the Joule heating method.

CRediT authorship contribution statement

Hanqing Yu: Writing – original draft, Conceptualization, Formal analysis. **Jianyu Li**: Investigation, Formal analysis. **Ni Yang**: Software, Formal analysis. **Dan Zhao**: Formal analysis. **Bo Yang**: Writing – review & editing, Supervision, Funding acquisition. **Yanqing Hou**: Writing – review & editing, Supervision. **Gang Xie**: Writing – review & editing, Supervision.

Declaration of competing interest

The authors declare that they have no known competing financial interests or personal relationships that could have appeared to influence the work reported in this paper.

Data availability

Data will be made available on request.

Acknowledgements

We gratefully acknowledge financial supports from the Open Project of State Key Laboratory of Advanced Metallurgy for Non-ferrous Metals (No. YSQH-ZYTS-24006).

Appendix A. Supplementary data

Figures S1-S3

References

[1] Liu, F.; Shi, C.; Guo, X.; He, Z.; Pan, L.; Huang, Z.-F.; Zhang, X.; Zou, J.-J. Rational Design of Better Hydrogen Evolution Electrocatalysts for Water Splitting: A Review. Advanced Science 2022, 9 (18), 2200307. https://doi.org/10.1002/advs.202200307.

[2] Liu, D.; Xu, G.; Yang, H.; Wang, H.; Xia, B. Y. Rational Design of Transition Metal Phosphide-Based Electrocatalysts for Hydrogen Evolution. Advanced Functional Materials 2023, 33 (7), 2208358. https://doi.org/10.1002/adfm.202208358.

[3] Gong, S.; Meng, Y.; Jin, Z.; Hsu, H.-Y.; Du, M.; Liu, F. Recent Progress on the Stability of Electrocatalysts under High Current Densities toward Industrial Water Splitting. ACS Catal. 2024, 14 (19), 14399–14435. https://doi.org/10.1021/acscatal.4c03700.

[4] Wu, Y.; Zhang, Y.; Wang, Y.; He, Z.; Gu, Z.; You, S. Potentiostatic Electrodeposited of Ni–Fe–Sn on Ni Foam Served as an Excellent Electrocatalyst for Hydrogen Evolution Reaction. International Journal of Hydrogen Energy 2021, 46 (53), 26930–26939. https://doi.org/10.1016/j.ijhydene.2021.05.189.

[5] Zhang, T.; He, Z.; Yin, L.; Gao, W.; Wang, Y. CoNi Alloy Nanoparticles Confined by N-Doped Carbon Matrix with Tailored d-Band Center for Electrocatalytic Hydrogen Evolution. Fuel 2024, 365, 131176. https://doi.org/10.1016/j.fuel.2024.131176.

[6] Jiao, M.; Chen, Z.; Zhang, X.; Mou, K.; Liu, L. Multicomponent N Doped Graphene Coating Co@Zn Heterostructures Electrocatalysts as High Efficiency HER Electrocatalyst in Alkaline Electrolyte. International Journal of Hydrogen Energy 2020, 45 (33), 16326–16336. https://doi.org/10.1016/j.ijhydene.2020.04.121.

[7] Li, B.; Li, Z.; Pang, Q.; Zhang, J. Z. Core/Shell Cable-like Ni3S2 Nanowires/N-Doped Graphene-like Carbon Layers as Composite Electrocatalyst for Overall Electrocatalytic Water Splitting. Chemical Engineering Journal 2020, 401, 126045. https://doi.org/10.1016/j.cej.2020.126045.

[8] Chen, Z.; Liu, X.; Xin, P.; Wang, H.; Wu, Y.; Gao, C.; He, Q.; Jiang, Y.; Hu, Z.;

Huang, S. Interface Engineering of NiS@MoS2 Core-Shell Microspheres as an Efficient Catalyst for Hydrogen Evolution Reaction in Both Acidic and Alkaline Medium. Journal of Alloys and Compounds 2021, 853, 157352. https://doi.org/10.1016/j.jallcom.2020.157352.

[9] Guo, X.; Duan, M.; Zhang, J.; Xi, B.; Li, M.; Yin, R.; Zheng, X.; Liu, Y.; Cao, F.; An, X.; Xiong, S. A General Self-Assembly Induced Strategy for Synthesizing 2D Ultrathin Cobalt-Based Compounds Toward Optimizing Hydrogen Evolution Catalysis. Advanced Functional Materials 2022, 32 (51), 2209397. https://doi.org/10.1002/adfm.202209397.

[10] Faraji, H.; Hemmati, K.; Mirabbaszadeh, K. Nickel-Based Nanosheets Array as a Binder Free and Highly Efficient Catalyst for Electrochemical Hydrogen Evolution Reaction. International Journal of Hydrogen Energy 2022, 47 (82), 34887–34897. https://doi.org/10.1016/j.ijhydene.2022.08.070.

[11] Luo, Y.; Zhang, Z.; Yang, F.; Li, J.; Liu, Z.; Ren, W.; Zhang, S.; Liu, B. Stabilized Hydroxide-Mediated Nickel-Based Electrocatalysts for High-Current-Density Hydrogen Evolution in Alkaline Media. Energy Environ. Sci. 2021, 14 (8), 4610–4619. https://doi.org/10.1039/D1EE01487K.

[12] Zheng, Y.; Li, Z.; Guo, H.; Liu, C.; Chen, Y.; Han, X.; Dong, L.; Zang, J. Vesicle-Shaped Co-Ni-S Designed by First Principles Screening and d-Band Center Control for Active Hydrogen Evolution. Fuel 2025, 382, 133743. https://doi.org/10.1016/j.fuel.2024.133743.

[13] Luong, D. X.; Bets, K. V.; Algozeeb, W. A.; Stanford, M. G.; Kittrell, C.; Chen, W.; Salvatierra, R. V.; Ren, M.; McHugh, E. A.; Advincula, P. A.; Wang, Z.; Bhatt, M.; Guo, H.; Mancevski, V.; Shahsavari, R.; Yakobson, B. I.; Tour, J. M. Gram-Scale Bottom-up Flash Graphene Synthesis. Nature 2020, 577 (7792), 647–651. https://doi.org/10.1038/s41586-020-1938-0.

[14] Wang, S.; Liu, Q.; Li, S.; Huang, F.; Zhang, H. Joule-Heating-Driven Synthesis of a Honeycomb-Like Porous Carbon Nanofiber/High Entropy Alloy Composite as an Ultralightweight Electromagnetic Wave Absorber. ACS Nano 2024, 18 (6), 5040–5050. https://doi.org/10.1021/acsnano.3c11408.

[15] Qiu, Y.; Hu, Z.; Li, H.; Ren, Q.; Chen, Y.; Hu, S. Hybrid Electrocatalyst Ag/Co/C via Flash Joule Heating for Oxygen Reduction Reaction in Alkaline Media. Chemical Engineering Journal 2022, 430, 132769. https://doi.org/10.1016/j.cej.2021.132769.

[16] Li, P.; Wei, W.; Li, J.; Liu, Y.; Fan, K.; Zong, L.; Wang, L. Flash Joule Heating Synthesis of Carbon Supported Ultrafine Metallic Heterostructures for High-Performance Overall Water Splitting. Journal of Alloys and Compounds 2023, 947, 169630. https://doi.org/10.1016/j.jallcom.2023.169630.

[17] Li, J. Flash Synthesis of Ultrafine and Active NiRu Alloy Nanoparticles on N-Rich Carbon Nanotubes via Joule Heating for Efficient Hydrogen and Oxygen Evolution Reaction. Journal of Alloys and Compounds 2023.

[18] Ding, H.; Liu, H.; Chu, W.; Wu, C.; Xie, Y. Structural Transformation of Heterogeneous Materials for Electrocatalytic Oxygen Evolution Reaction. Chem. Rev. 2021, 121 (21), 13174–13212. https://doi.org/10.1021/acs.chemrev.1c00234.

[19] Li, H.; Lai, J.; Li, Z.; Wang, L. Multi-Sites Electrocatalysis in High-Entropy Alloys. Advanced Functional Materials 2021, 31 (47), 2106715. https://doi.org/10.1002/adfm.202106715.

[20] Zheng, X.; Liu, Y.; Yang, Y.; Song, Y.; Deng, P.; Li, J.; Liu, W.; Shen, Y.; Tian, X. Recent Advances in Cadmium Sulfide-Based Photocatalysts for Photocatalytic Hydrogen Evolution. Renewables 2023. https://doi.org/10.31635/renewables.022.202200001.

[21] Ahirrao, D. J.; Pal, A. K.; Singh, V.; Jha, N. Nanostructured Porous Polyaniline (PANI) Coated Carbon Cloth (CC) as Electrodes for Flexible Supercapacitor Device. Journal of Materials Science & Technology 2021, 88, 168–182. https://doi.org/10.1016/j.jmst.2021.01.075.

[22] Wang, Z.; Zhang, M.; Ma, W.; Zhu, J.; Song, W. Application of Carbon Materials in Aqueous Zinc Ion Energy Storage Devices. Small 2021, 17 (19), 2100219. https://doi.org/10.1002/smll.202100219.

[23] Peng, Y.; Sanati, S.; Morsali, A.; García, H. Metal–Organic Frameworks as Electrocatalysts. Angewandte Chemie International Edition 2023, 62 (9),

e202214707. https://doi.org/10.1002/anie.202214707.

[24] Wu, F.; Zeng, L.; Pei, A.; Feng, Y.; Zhu, L. N, P Co-Doped Graphene-Supported Monometallic Nanoparticles for Highly Efficient Hydrogen Evolution by Acid Electrolysis of Water. J. Mater. Chem. A 2024, 12 (17), 10300–10306. https://doi.org/10.1039/D3TA07750K.

[25] Vedrtnam, A.; Sharma, S. P. Study on the Performance of Different Nano-Species Used for Surface Modification of Carbon Fiber for Interface Strengthening. Composites Part A: Applied Science and Manufacturing 2019, 125, 105509. https://doi.org/10.1016/j.compositesa.2019.105509.

[26] Wang, B.; Yao, Y.; Yu, X.; Wang, C.; Wu, C.; Zou, Z. Understanding the Enhanced Catalytic Activity of High Entropy Alloys: From Theory to Experiment. Journal of Materials Chemistry A 2021, 9 (35), 19410–19438. https://doi.org/10.1039/D1TA02718B.

[27] Zheng, X.; Yang, Y.; Song, Y.; Ma, Z.; Gao, Q.; Liu, Y.; Li, J.; Wu, X.; Wang, X.; Mao, W.; Liu, W.; Shen, Y.; Tian, X. Recent Advances in Photocatalytic Hydrogen Evolution of AgIn5S8-Based Photocatalysts. Interdisciplinary Materials 2023, 2 (5), 669–688. https://doi.org/10.1002/idm2.12120.

[28] Ye, H.; Li, L.; Liu, D.; Fu, Q.; Zhang, F.; Dai, P.; Gu, X.; Zhao, X. Sustained-Release Method for the Directed Synthesis of ZIF-Derived Ultrafine Co-N-C ORR Catalysts with Embedded Co Quantum Dots. ACS Appl. Mater. Interfaces 2020, 12 (52), 57847–57858. https://doi.org/10.1021/acsami.0c16081.

[29] Pei, A.; Li, G.; Zhu, L.; Huang, Z.; Ye, J.; Chang, Y.-C.; Osman, S. M.; Pao, C.-W.; Gao, Q.; Chen, B. H.; Luque, R. Nickel Hydroxide-Supported Ru Single Atoms and Pd Nanoclusters for Enhanced Electrocatalytic Hydrogen Evolution and Ethanol Oxidation. Advanced Functional Materials 2022, 32 (51), 2208587. https://doi.org/10.1002/adfm.202208587.

[30] Wang, J.; Xin, S.; Xiao, Y.; Zhang, Z.; Li, Z.; Zhang, W.; Li, C.; Bao, R.; Peng, J.; Yi, J.; Chou, S. Manipulating the Water Dissociation Electrocatalytic Sites of Bimetallic Nickel-Based Alloys for Highly Efficient Alkaline Hydrogen Evolution. Angewandte Chemie International Edition 2022, 61 (30), e202202518.

https://doi.org/10.1002/anie.202202518.

[31] Wang, Z.; Shen, S.; Wang, J.; Zhong, W. Modulating the D‐Band Center of Electrocatalysts for Enhanced Water Splitting. Chemistry A European J 2024, e202402725. https://doi.org/10.1002/chem.202402725.

[32] Jiao, S.; Fu, X.; Huang, H. Descriptors for the Evaluation of Electrocatalytic Reactions: d‐Band Theory and Beyond. Adv Funct Materials 2022, 32 (4), 2107651. https://doi.org/10.1002/adfm.202107651.

[33] Bi, S.; Xu, H.; Xue, M.; Jin, L.; Geng, Z.; Zhang, C. Stimulated pH-Dependence Phosphorus Platinum–Nickel Alloy Cluster as Hydrogen Generation Electrocatalyst in Alkaline Solution. Energy Technology 2022, 10 (8), 2200380. https://doi.org/10.1002/ente.202200380.

[34] Xie, C.; Yan, D.; Chen, W.; Zou, Y.; Chen, R.; Zang, S.; Wang, Y.; Yao, X.; Wang, S. Insight into the Design of Defect Electrocatalysts: From Electronic Structure to Adsorption Energy. Materials Today 2019, 31, 47–68. https://doi.org/10.1016/j.mattod.2019.05.021.

[35] Agbo, P.; Danilovic, N. An Algorithm for the Extraction of Tafel Slopes. J. Phys. Chem. C 2019, 123 (50), 30252–30264. https://doi.org/10.1021/acs.jpcc.9b06820.

[36] McCrory, C. C. L.; Jung, S.; Peters, J. C.; Jaramillo, T. F. Benchmarking Heterogeneous Electrocatalysts for the Oxygen Evolution Reaction. J. Am. Chem. Soc. 2013, 135 (45), 16977–16987. https://doi.org/10.1021/ja407115p.

[37] Gultom, N. S.; Silitonga, M. Z.; Kuo, D.-H. Bimetallic Cobalt–Nickel Electrode Made by a Sputtering Technique for Electrocatalytic Hydrogen Evolution Reaction: Effect of Nickel Ratios. ACS Appl. Energy Mater. 2022, 5 (7), 8658–8668. https://doi.org/10.1021/acsaem.2c01177.

[38] Björketun, M. E.; Tripkovic, V.; Skúlason, E.; Rossmeisl, J. Modeling of the Symmetry Factor of Electrochemical Proton Discharge via the Volmer Reaction. Catalysis Today 2013, 202, 168–174. https://doi.org/10.1016/j.cattod.2012.05.044.

[39] Bhardwaj, M.; Balasubramaniam, R. Uncoupled Non-Linear Equations Method for Determining Kinetic Parameters in Case of Hydrogen Evolution Reaction Following Volmer–Heyrovsky–Tafel Mechanism and Volmer–Heyrovsky

Mechanism. International Journal of Hydrogen Energy 2008, 33 (9), 2178–2188. https://doi.org/10.1016/j.ijhydene.2008.02.027.

[40] He, Y.; Kang, Z.; Li, J.; Li, Y.; Tian, X. Recent Progress of Manganese Dioxide Based Electrocatalysts for the Oxygen Evolution Reaction. Industrial Chemistry & Materials 2023, 1 (3), 312–331. https://doi.org/10.1039/D3IM00034F.

[41] Pei, A.; Xie, R.; Zhang, Y.; Feng, Y.; Wang, W.; Zhang, S.; Huang, Z.; Zhu, L.; Chai, G.; Yang, Z.; Gao, Q.; Ye, H.; Shang, C.; Hui Chen, B.; Guo, Z. Effective Electronic Tuning of Pt Single Atoms via Heterogeneous Atomic Coordination of (Co,Ni)(OH) 2 for Efficient Hydrogen Evolution. Energy & Environmental Science 2023, 16 (3), 1035–1048. https://doi.org/10.1039/D2EE02785B.

[42] Wang, Y.; Pan, Y.; Zhang, X.; Huang, X.; Li, T.; Liu, S.; Tang, S.; Sun, Y.; Shao, B.; Liu, Z. Defect Engineering Boosting PMS Activation Activity on Cobalt Polyphthalocyanine: Promoting Co(IV)=O Formation and Enhancing 1O2 Selectivity. Separation and Purification Technology 2025, 357, 130085. https://doi.org/10.1016/j.seppur.2024.130085.

[43] Pan, Y.; Zhang, X.; Wu, T.; Shao, B.; Li, T.; He, Q.; Chen, Z.; Zhou, L.; Liu, S.; Huang, X.; Liu, Z. Application of 3D Hierarchical Porous NiCo-Spinel Nanosheet Array for Enhancement of Synergistic Activation of Peroxymonosulfate: Degradation, Intermediates, Mechanism and Degradation Pathway of Tetracycline. Chemical Engineering Journal 2024, 481, 148506. https://doi.org/10.1016/j.cej.2023.148506.

[44] Wu, T.; Liu, Z.; Shao, B.; He, Q.; Pan, Y.; Zhang, X.; Sun, J.; He, M.; Ge, L.; Cheng, C.; Hu, T. Enhanced Piezo-Photocatalytic Degradation of Organic Pollutants by Cambered Wall Lamellar Structure of Porous Tubular g-C3N4. Nano Energy 2024, 120, 109137. https://doi.org/10.1016/j.nanoen.2023.109137.

[45] Wu, T.; Liang, Q.; Tang, L.; Tang, J.; Wang, J.; Shao, B.; Gong, S.; He, Q.; Pan, Y.; Liu, Z. Construction of a Novel S-Scheme Heterojunction Piezoelectric Photocatalyst V-BiOIO3/FTCN and Immobilization with Floatability for Tetracycline Degradation. Journal of Hazardous Materials 2023, 443, 130251. https://doi.org/10.1016/j.jhazmat.2022.130251.

Declaration of interests

☒ The authors declare that they have no known competing financial interests or personal relationships that could have appeared to influence the work reported in this paper.

Highlights

- A method for preparing cobalt-nickel nanoalloy heterostructures on carbon fiber surfaces via ultrafast Joule heating has been proposed.
- The electrochemical performance of cobalt-nickel nanoalloy heterostructures on carbon fibers was studied experimentally and applied to electrocatalytic hydrogen evolution reactions.
- The potential of Joule flash heating technology for rapidly constructing efficient heterostructures was demonstrated, offering new insights for developing integrated water-splitting electrocatalysts.